


RESEARCH ARTICLE

Exosomal circ-AHCY promotes glioblastoma cell growth via Wnt/ β -catenin signaling pathway

Yuhui Li^{1,*}, Xuan Zheng^{2,*}, Jiangong Wang³, Mingyang Sun¹, Dan Li², Zhuo Wang², Jingwu Li², Yufeng Li² & Yongliang Liu¹ ¹Department of Neurosurgery, Tangshan People's Hospital, Tangshan, Hebei, 063001, China²The Cancer Institute, Tangshan People's Hospital, Tangshan, Hebei, 063001, China³Department of Chemoradiotherapy, Tangshan People's Hospital, Tangshan, Hebei, 063001, China

Correspondence

Jingwu Li and Yufeng Li, The Cancer Institute, Tangshan People's Hospital, No.65 Shengli Road, Lunan District, Tangshan, Hebei 063001, China. Tel: 86 18932517973; Fax: 86 315 2875796; and Tel: 86 15383055796; Fax: 86 315 2875796; E-mail: tslijingwu@163.com and yufeng_li@tsrmyy.cn

Yongliang Liu, Department of Neurosurgery, Tangshan People's Hospital, No.65 Shengli Road, Lunan District, Tangshan, Hebei 063001, China. Tel: 86 18230300953; Fax: 86 315 2875796 E-mail: s_c_2000@163.com

Funding information: 2020 Talent Project Fund of Tangshan : A202006017 Fund of Key Laboratory of Hebei Province : SZX2020043 2022 Science and Technology Planning Project Fund of Tangshan : 22130202H

Received: 18 November 2022; Revised: 12 January 2023; Accepted: 31 January 2023

Annals of Clinical and Translational Neurology 2023; 10(6): 865–878

doi: 10.1002/acn3.51743

*Yuhui Li and Xuan Zheng are Co-first authors.

Abstract

Background: Glioblastoma (GBM) is the most aggressive brain tumor. Reportedly, circular RNAs (circRNAs) participate in regulation of the development and progression of diverse cancers, including GBM. **Methods:** Dysregulated circRNAs in GBM tissues were screened out from GEO database. The expression of candidate circRNAs in GBM cells was measured by qRT-PCR. Loss-of function assays, including colony formation assay, EdU assay, TUNEL assay, and flow cytometry analysis were conducted to determine the effects of circ-AHCY knockdown on GBM cell proliferation and apoptosis. Animal study was further used to prove the inhibitory effect of circ-AHCY silencing on GBM cell growth. Mechanistic experiments like luciferase reporter, RNA pull-down and RNA-binding protein immunoprecipitation (RIP) assays were performed to unveil the downstream molecular mechanism of circ-AHCY. Nanosight Nanoparticle Tracking Analysis (NTA) and PKH67 staining were applied to identify the existence of exosomes. **Results:** Circ-AHCY was confirmed to be highly expressed in GBM cells. Circ-AHCY silencing suppressed GBM cell proliferation both in vitro and in vivo. Mechanistically, circ-AHCY activates Wnt/ β -catenin signaling pathway by sequestering miR-1294 to up-regulate MYC which activated CTNNB1 transcription. It was also found that circ-AHCY recruited EIF4A3 to stabilize TCF4 mRNA. Enhanced levels of TCF4 and β -catenin contributed to the stability of TCF4/ β -catenin complex. In turn, TCF4/ β -catenin complex strengthened the transcriptional activity of circ-AHCY. Exosomal circ-AHCY derived from GBM cells induced abnormal proliferation of normal human astrocytes (NHAs). **Conclusion:** Exosomal circ-AHCY forms a positive feedback loop with Wnt/ β -catenin signaling pathway to promote GBM cell growth.

Introduction

Glioblastoma (GBM) is the most aggressive primary brain tumor, characterized by variable histopathology as well as unfavorable clinical outcomes and prognosis.^{1,2} Current treatments combine surgical resection, chemotherapy, and radiotherapy. Rapid progression of GBM, resistance to therapy, and inevitable recurrence have been ascribed to multiple typical factors, including heterogeneity of inter-

and intra-tumoral, propensity to infiltrate essential brain structures, and regeneration of treatment-resistant cancer stem cells.³ As these changes exist, GBM complicates the development of effective therapeutic approaches.⁴

Circular RNAs (circRNAs), covalently closed RNA transcripts, have been identified to engage in varied physiological and pathological processes.⁵ For instance, circPTK2 has been uncovered to serve as a cancer suppressor in GBM, its over-expression inhibited GBM cell migration and invasion.⁶

Hsa_circ_0072309 has also been verified to impede proliferation and invasion of GBM, which supported this gene to be a potential therapeutic target against GBM.⁷

Emerging evidence has been revealed that circRNAs are able to regulate GBM evolution via diverse signaling pathways. As reported by Xin et al., hsa_circ_0067934 up-regulation contributes to GBM progression via activation PI3K/AKT signaling pathway.⁸ Circ_PTN has also been corroborated to promote cisplatin (DDP) resistance of GBM cells through activating PI3K/AKT signaling pathway.⁹ Moreover, it has been identified that circRNAs serve as competing endogenous RNAs (ceRNAs), and can compete with protein-coding messenger RNAs (mRNAs) for shared microRNAs (miRNAs). CeRNA activity represents a common form of gene expression at the post-transcriptional level, depending on multiple factors including subcellular distribution of ceRNA components and binding affinity of miRNAs to their sponges.^{10,11} According to published research work, hsa_circ_0006168 is allowed to influence GBM proliferation and motility via sequestering miR-628-5p and up-regulating IFG1R.¹² CircHECTD1 has also been unveiled to regulate GBM cell proliferation and migration via targeting miR-320-5p/SLC2A1 axis.¹³

In this study, we first utilized GEO dataset (GSE146463) to screen candidate circRNAs which are highly expressed in GBM cells as our research subject. Through mechanistic analyses, we tried to figure out whether a certain signaling pathway or ceRNA network was involved in the regulation of our subject circRNA. Our findings were expected to enrich the understanding of molecular mechanism in GBM and providing evidence for developing the promising biomarkers of GBM treatment.

Materials and Methods

Cell culture

Normal human astrocytes (NHAs) and five human GBM cell lines including LN229, U87, A172, T98 and U251, as well as human embryonic kidney cell line 293T, were obtained from American Type Culture Collection (Manassas, VA, USA) and kept in in DMEM supplemented with 10% fetal bovine serum. The environment was maintained at 37°C with 5% CO₂.

Cell transfection

Short hairpin RNAs (shRNAs) targeting circ-AHCY, MYC, TEAD1 TCF4, EIF4A3 were respectively designed for knockdown of targeted genes, with sh-NC as negative control. For miRNA overexpression, miR-3918 mimics, miR-1294 mimics and miR-1249-3p mimics were synthesized, while miR-1294 inhibitor was designed for miR-1294

inhibition. Mimics NC and inhibitor NC were taken as negative control, separately. Moreover, pcDNA3.1-circ-AHCY, pcDNA3.1-MYC and pcDNA3.1-TCF4 were utilized for gene overexpression, with empty pcDNA3.1 as negative control. Plasmid transfection into cells was performed by means of Lipofectamine 2000. Cells with stable transfection were collected 48 h post transfection.

Real-time reverse transcription-PCR (qRT-PCR)

With the application of TRIzol Reagent, total RNA was obtained for reverse transcription into cDNA using RevertAid First Strand cDNA Synthesis Kit. SYBR Green PCR Master Mix was used to perform PCR analysis. Relative expression levels were determined by 2^{-ΔΔCt} method. GAPDH or U6 was used as an endogenous control.

Cell counting kit-8 (CCK-8) assay

CCK-8 Kit was utilized to assess cell viability as per the standard protocol. Cells were plated into 96-well plates for incubation at 37°C with 5% CO₂. Absorbance at 450 nm was observed using a microplate reader.

Colony formation assay

In brief, 20,000–80,000 stably transfected cells were added into 6-well plates and incubated for 14 days. Cells were then fixed in 4% paraformaldehyde, followed by staining with 0.5% crystal violet. The stained cell colonies were counted manually.

5-Ethynyl-2'-deoxyuridine (EdU)

EdU Imaging Kit was utilized to assess cell proliferation based on the supplier's recommendations. The transfected cells were seeded into 96-well plates, followed by treatment with EdU solution for 23 h at 37°C. Subsequently, cells were subjected to fixation with 4% paraformaldehyde and nuclear staining with DAPI. Lastly, EdU positive cells were observed using fluorescence microscopy.

Terminal-deoxynucleotidyl transferase mediated nick end labeling (TUNEL)

TUNEL Kit was employed for TUNEL assay following the supplier's suggestions. Cells were seeded in 96-well plates and rinsed in PBS post transfection. Then, cells were fixed by 4% paraformaldehyde at 37°C and incubated with TdT reaction mix. DAPI was utilized for nuclear staining. Cell apoptosis was analyzed under a laser scanning confocal microscope.

Flow cytometry analysis

Cell apoptosis was evaluated via flow cytometry analysis. Transfected cells were dyed by Annexin V/FITC and propidium iodide (PI) at room temperature in the dark for 15 min. The apoptotic cells were examined via flow cytometry following the manufacturer's recommendations.

Animal experiment

Four to five weeks old male nude mice were commercially attained from Model Animal Research Center of Nanjing University. For the subcutaneous implantation model, LN229 cells stably transfected with sh1-circ-AHCY or sh-NC were inoculated subcutaneously in the right thigh root of the mice. Tumor volume was calculated every 3 days based on the formula: $(\text{length} \times \text{width}^2)/2$, and tumors were weighed 4 weeks later when all mice were sacrificed. The experiments were approved by the Ethics Committee of Tangshan People's Hospital. Tumor sections were prepared for subsequent TUNEL assay and immunohistochemistry (IHC) analysis.

IHC

Samples were cut to an appropriate size, followed by fixation with 4% paraformaldehyde. Subsequently, the paraformaldehyde-fixed samples were subjected to dehydration and paraffin-embedding before being sectioned into thin slices. Then, the sections were incubated with primary antibody against Ki67 (anti-Ki67) and PCNA (anti-PCNA) at 4°C overnight. After PBS washing, secondary antibody was added for 1 h of incubation at room temperature. Images were captured using fluorescence microscopy.

Fluorescence in situ hybridization (FISH)

Fluorescent in situ Hybridization Kit was utilized to perform FISH assay. Subsequent to fixation with 4% paraformaldehyde at room temperature, cells were permeabilized using TritonX-100. After PBS washing, cells were co-cultured with FISH probe against circ-AHCY. Detection of Cy3 labeled probe (Takara, Tokyo, Japan) against circ-AHCY was performed by FISH in GW4869 (Takara)-treated NHA cells co-cultured with GBM cell-derived exosomes. DAPI was used to dye the nucleus. Finally, images were obtained using confocal microscope.

Subcellular fractionation assay

Cells were rinsed in pre-cooled PBS for 2 times, then centrifuged and cultured in lysis buffer. The cell nucleus and cell cytoplasm were separately extracted by use of

PARIS™ Kit. Level of circ-AHCY was assayed in both fractions through qRT-PCR.

Luciferase reporter assay

To analyze the interaction between different factors, pmirGLO and pGL3 vectors were obtained for construction of luciferase reporters including pmirGLO-CTNNB1 3'UTR, pGL3-CTNNB1 promoter, pmirGLO-circ-AHCY, pmirGLO-AHCY-WT/Mut, pmirGLO-MYC 3'UTR-WT/Mut or pGL3-CTNNB1 promoter-WT/Mut1/Mut2/Mut1+2. These reporters were respectively transfected into 293T cells with indicated gene knockdown or overexpression. Dual-Luciferase Reporter Assay System (Promega, USA) was applied for the detection of luciferase activity.

Signal finder reporter array

To identify the specific signaling pathway modulated by circ-AHCY, we use the Signal Finder Pathway Arrays (336841, QIAGEN, Dusseldorf, Germany) to detect the activity of the downstream transcription factors of specific pathways. At the first day, the GBM cells were seeded onto the transfection complexes which were constituted with the Attractene transfection reagent (Qiagen) and test nucleic acids. Twenty-four hours after transfection, cells were added with resveratrol and incubated for another 6 h before developing the assay. The luciferase assay was carried out using the Dual-Luciferase Reporter Assay System (Promega) following the manufacturer's protocol for developing the assay.

Western blot

Protein lysates were obtained using RIPA buffer. Isolation of total protein was performed using PROTOT-1KT, and protein concentration was examined by Bradford Protein Assay Kit. The isolated total protein was treated with SDS-PAGE for separation and subsequently transferred onto PVDF membranes. Subsequently, the membranes were sealed by 5% non-fat milk and incubated with specific primary antibodies including Anti-β-actin, Anti-β-catenin, Anti-c-Myc, Anti-VEGFA, Anti-MYC, Anti-TCF4, Anti-EIF4A3, Anti-CD63, Anti-CD81 and Anti-TSG101 overnight at 4°C. Then, secondary antibodies were added for cultivation. Lastly, the blots were detected via enhanced chemiluminescence (ECL) detection system.

RNA-binding protein immunoprecipitation (RIP)

Cell lysates were cultured with Anti-Ago2, Anti-EIF4A3 or negative control Anti-IgG conjugated with magnetic beads. The immunoprecipitated RNAs were isolated and

subsequently examined via qRT-PCR for quantification of target gene enrichment.

RNA pull-down assay

Biotinylated circ-AHCY-WT/Mut, TCF4 sense or Anti-sense, miR-1294-WT/Mut were designed and constructed. The probes were then cultivated with streptavidin magnetic beads to form probe-coated beads. Cell lysates were mixed with probe-coated beads for overnight incubation. RNAs and proteins pulled down by biotinylated probes were subjected to qRT-PCR or western blot.

Chromatin immunoprecipitation (ChIP)

ChIP assay was done using EZ-ChIP Kit. The cross-linked chromatin samples were fragmented for immunoprecipitation with Anti-MYC, Anti-TCF4 or Anti-IgG antibody at 4°C overnight. Afterwards, the samples were incubated with magnetic beads. The immunoprecipitated DNA was purified and detected by qPCR analysis.

Exosome isolation, identification and labeling

The culture medium from LN229 and A172 cells was harvested, centrifuged at 300g for 10 min, 1200g for 20 min, and 10,000g for 30 min to remove cells and debris. The supernatant was ultracentrifuged at 200,000g for 2 h. Then the exosome pellet was resuspended in PBS and then the exosomes were harvested for RNA isolations. Exosome markers including CD63, CD81 and TSG101 were detected via western blot for exosome identification. Exosome quantification was determined via Nanosight Nanoparticle Tracking Analysis (NTA) as previously described.¹⁴ Also, to detect the existence of exosomes, the exosomes were labeled with green PKH67 fluorescence. DAPI was employed for nuclear counterstain. The fluorescence was examined via confocal microscope.

GW4869 treatment

GW4869 (10 μM) was used to inhibit exosome release in LN229 and A172 cells as well as NHA cells co-cultured with GBM cell-derived exosomes.

Statistical analysis

All experiments were triplicated and the experimental results were expressed as the mean ± SD. Student's t-test or one-way or two-way analysis of variance (ANOVA) was applied for difference comparison between groups in

vitro and in vivo. Data were considered as statistical significance with a *p* value below 0.05.

Results

Circ-AHCY has a high expression in GBM cells

At the very beginning, we searched GEO dataset (GSE146463) and selected top 10 circRNAs that were most significantly overexpressed in GBM cells (Fig. 1A). Comparing with NHAs, we noticed only hsa_circ_0059914 demonstrated a high expression in GBM cells, especially in LN229 and A172 cells (Fig. 1B). Based on the above findings, hsa_circ_0059914 was decided as the research subject, and LN229 and A172 cells were involved in the following investigation. As presented in Fig. 1C, hsa_circ_0059914 was derived from its host gene AHCY via back-splicing. The following qRT-PCR analysis indicated that circ-AHCY expression was hardly affected in GBM cells upon RNase R/ActD treatment (Fig. 1D,E), representing that circ-AHCY possesses a more stable structure than GAPDH. In brief, circ-AHCY is highly expressed in GBM cells and has a stable circular structure.

Circ-AHCY knockdown suppresses GBM progression in vitro and in vivo

Prior to investigating the biological role of circ-AHCY, we confirmed the high efficacy of sh1/2/3-circ-AHCY (Fig. 2A). Loss-of-function assays in vitro demonstrated that circ-AHCY deficiency repressed proliferation (Fig. 2B–D) and apoptosis (Fig. 2E,F) of GBM cells. In addition, we performed rescue experiments to further verify the impact of circ-AHCY on GBM cell proliferation and apoptosis. It was found that overexpression of circ-AHCY could restore the suppression on GBM cell proliferation caused by circ-AHCY knockdown; meanwhile, up-regulation of circ-AHCY could counteract the promotion on cell apoptosis induced by circ-AHCY deficiency (Fig. S1A,B). We also constructed xenograft model, and in vivo study revealed that xenograft tumor growth was inhibited on account of circ-AHCY depletion (Fig. 2G). IHC images presented that the percentage of Ki-67 or PCNA positive cells was reduced and that of TUNEL positive cells was increased in sh1-circ-AHCY group compared to sh-NC group (Fig. 2H). To sum up, circ-AHCY down-regulation results in the inhibition of GBM cell and tumor growth.

Circ-AHCY facilitates CTNNB1 transcription to activate Wnt/β-catenin signaling pathway

CircRNAs have been reported to exert their biological functions in cancer via regulating signaling pathways.^{5,8,9}

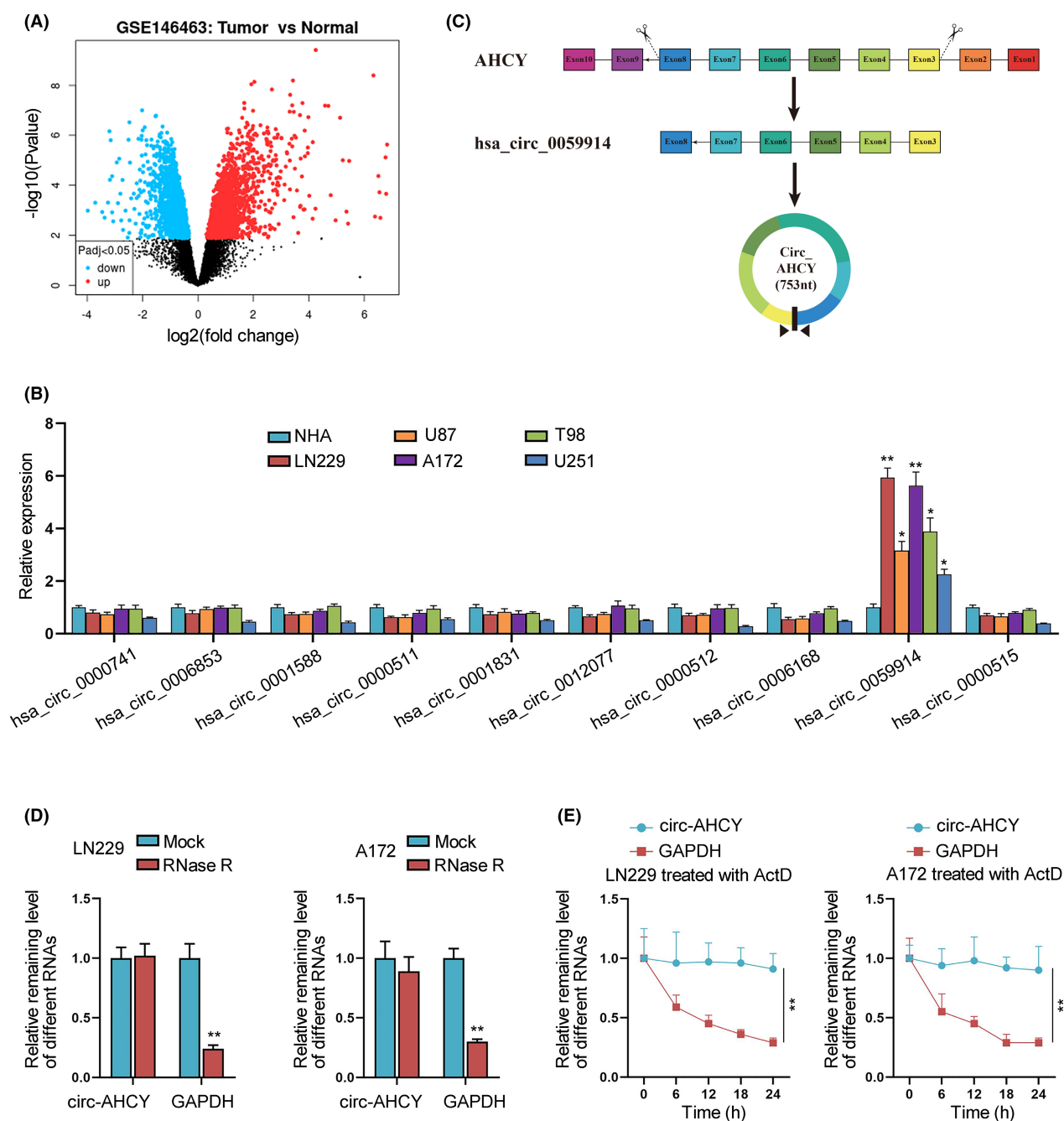


Figure 1. Circ-AHCY is up-regulated in GBM cells. (A) GSE146463 dataset predicted the up-regulated circRNAs in GBM cells in comparison with normal cells. (B) The expressions of the top 10 most up-regulated circRNAs were examined via qRT-PCR in different GBM cell lines as well as in NHA cells. (C) The circular formation of circ-AHCY. (D) Circ-AHCY and GAPDH was treated by RNase R and the remaining levels were unclosed. (E) After ActD treatment, remaining level of circ-AHCY and GAPDH in LN229 cells was analyzed. $*p < 0.05$, $**p < 0.01$.

In this section, we firstly detected the subcellular distribution of circ-AHCY in LN229 and A172 cells via FISH and subcellular fractionation assays. It was observed that circ-AHCY was mainly distributed in cytoplasm of GBM cells (Fig. 3A,B). With the use of Signal Finder Reporter

Array, we found that the activity of Wnt signaling pathway was significantly decreased by circ-AHCY depletion (Fig. 3C). Western blots presented that circ-AHCY deficiency led to a decline of β -catenin and c-Myc protein levels (Fig. 3D). Subsequently, qRT-PCR results indicated

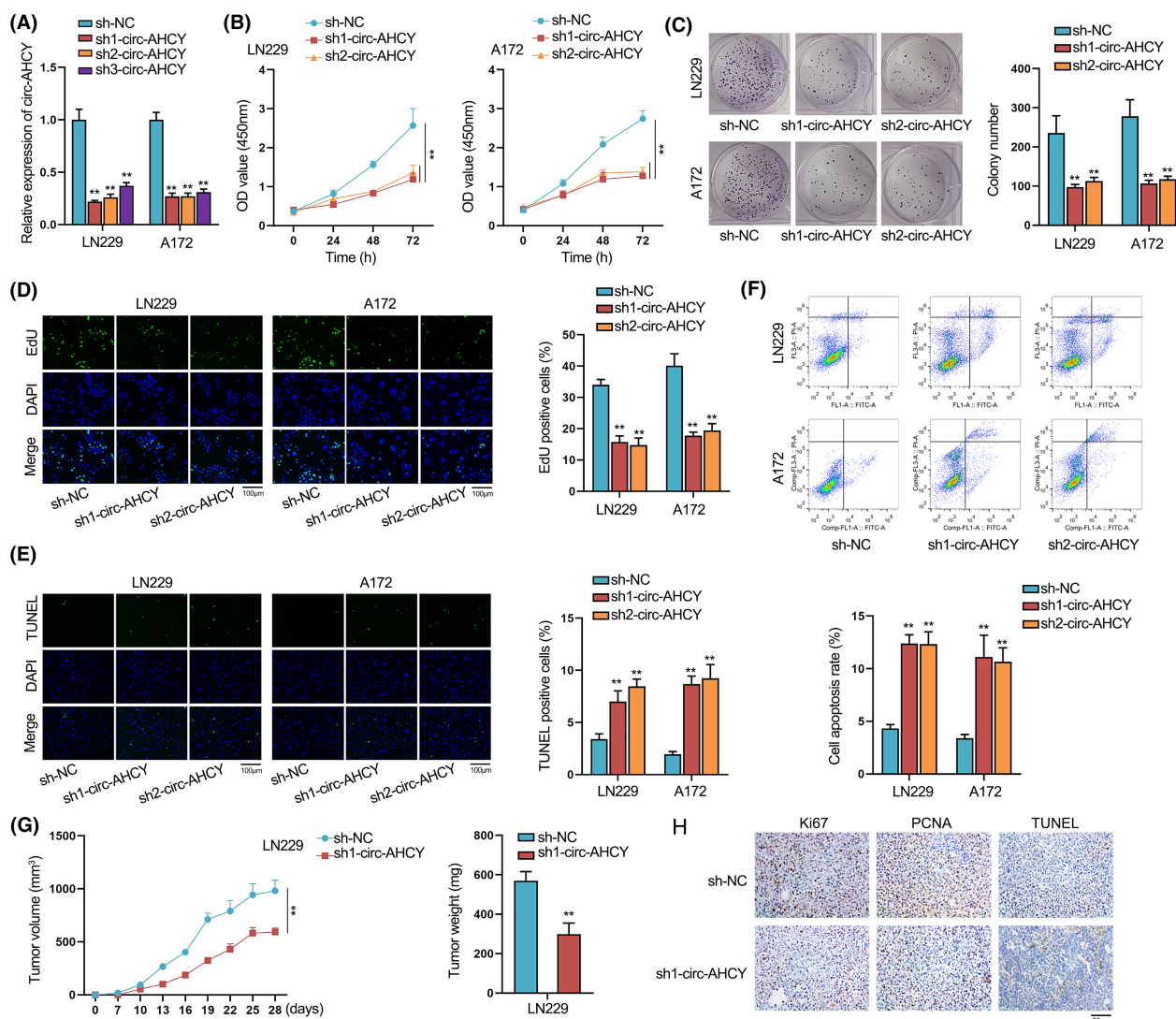


Figure 2. GBM cell growth is inhibited due to circ-AHCY depletion. (A) Circ-AHCY was interfered after sh1/2/3-circ-AHCY was transfected into GBM cells. (B–D) CCK-8, colony formation and EdU assays were performed to analyze cell proliferation after circ-AHCY silence. Scale bar = 100 μm. (E and F) TUNEL and flow cytometry analyzed cell apoptosis after circ-AHCY silence. Scale bar = 100 μm. (G) Tumor growth was monitored by measuring tumor volumes every 3 days, and tumors were weighed after removal on day 28. (H) IHC detected Ki67-positive, PCNA-positive and TUNEL-positive cells in tumor tissues of different groups. Scale bar = 50 μm. ***p* < 0.01.

that circ-AHCY knockdown lessened the expression of CTNNB1 (the mRNA of β -catenin) (Fig. 3E). Through luciferase reporter assay, we found that the activity of CTNNB1 promoter was diminished after circ-AHCY knockdown (Fig. 3F). In addition, although circ-AHCY could be detected in RISC (Fig. 3G), the activity of CTNNB1 3'UTR was hardly affected upon circ-AHCY depletion (Fig. 3H). Based on these findings, we concluded that circ-AHCY did not directly regulate CTNNB1 through ceRNA mode, but improved the transcriptional activity of CTNNB1 promoter instead. To summarize, circ-AHCY promotes CTNNB1 transcription to further activate Wnt/ β -catenin signaling pathway in GBM cells.

Circ-AHCY transcriptionally activates CTNNB1 via miR-1294/MYC axis

In this section, we tried to complete circ-AHCY-centered ceRNA network. StarBase website (<https://starbase.sysu.edu.cn/>) was utilized to project candidate miRNAs binding with circ-AHCY. Under the condition of strict stringency ≥ 5 , miR-3918, miR-1294, and miR-1249-3p stood out as the miRNA candidates involved in the following luciferase reporter assay. As shown in Fig. 4A, only miR-1294 overexpression declined the luciferase activity of circ-AHCY, for which miR-3918 and miR-1249-3p were excluded from this study. We further confirmed the

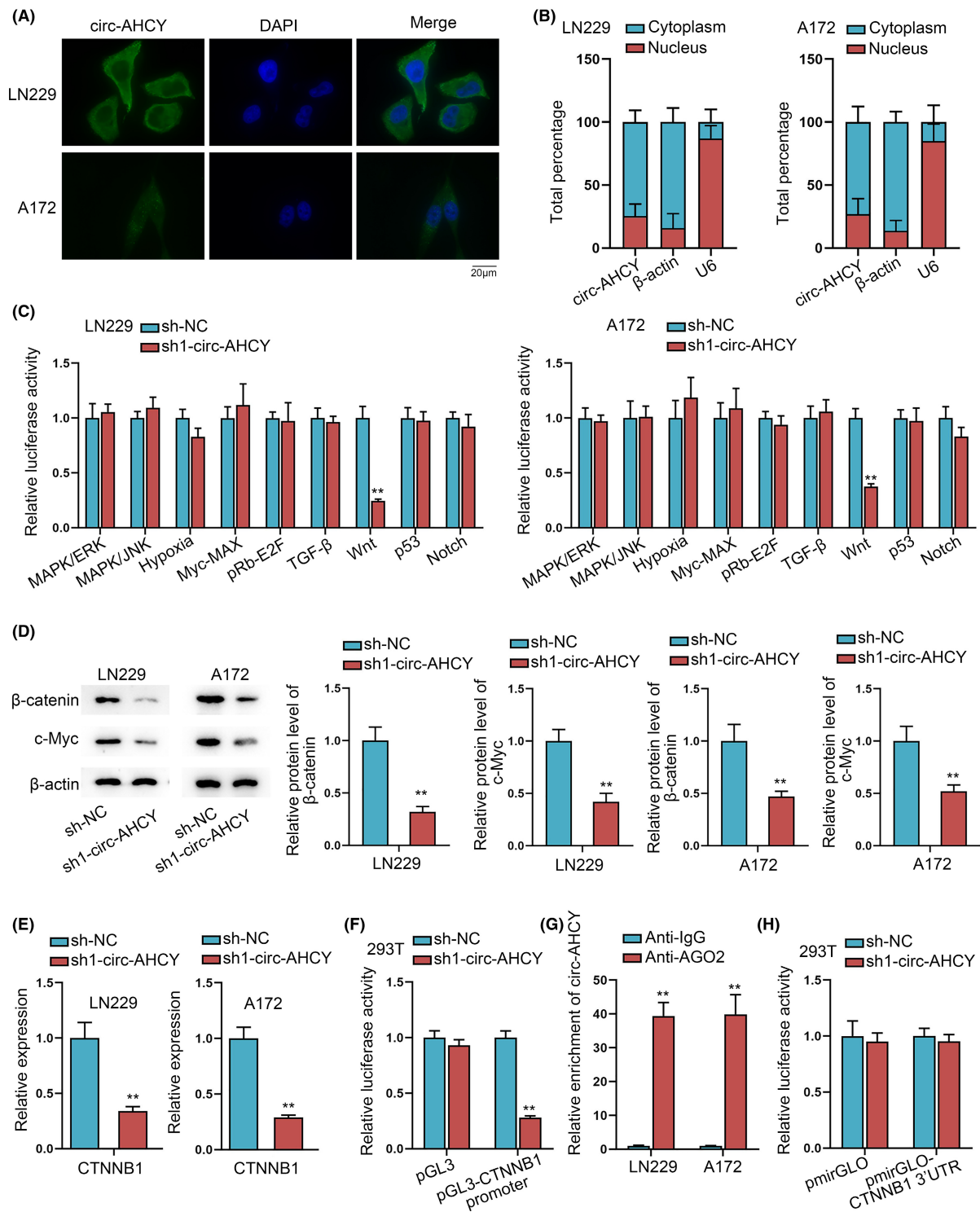


Figure 3. Circ-AHCY activates Wnt/β-catenin pathway via transcriptionally modulating CTNNB1. (A) FISH assay detected circ-AHCY distribution in LN229 and A172 cells. Scale bar = 20 μm. (B) Subcellular fractionation and qRT-PCR jointly revealed circ-AHCY level in different cellular parts. (C) The luciferase activities of different signaling pathways were detected with luciferase activity assay. (D) Key proteins in Wnt signaling pathway were measured through western blot after circ-AHCY depletion. (E) CTNNB1 expression after circ-AHCY knockdown was detected by qRT-PCR. (F) Luciferase activity of pGL3-CTNNB1 promoter was detected in 293T cells with co-transfection of sh1-circ-AHCY. (G) RIP assay analyzed the enrichment of circ-AHCY in RISC. (H) Luciferase activity of pmirGLO-CTNNB1 3'UTR after circ-AHCY silence in 293T cells was detected. ** $p < 0.01$.

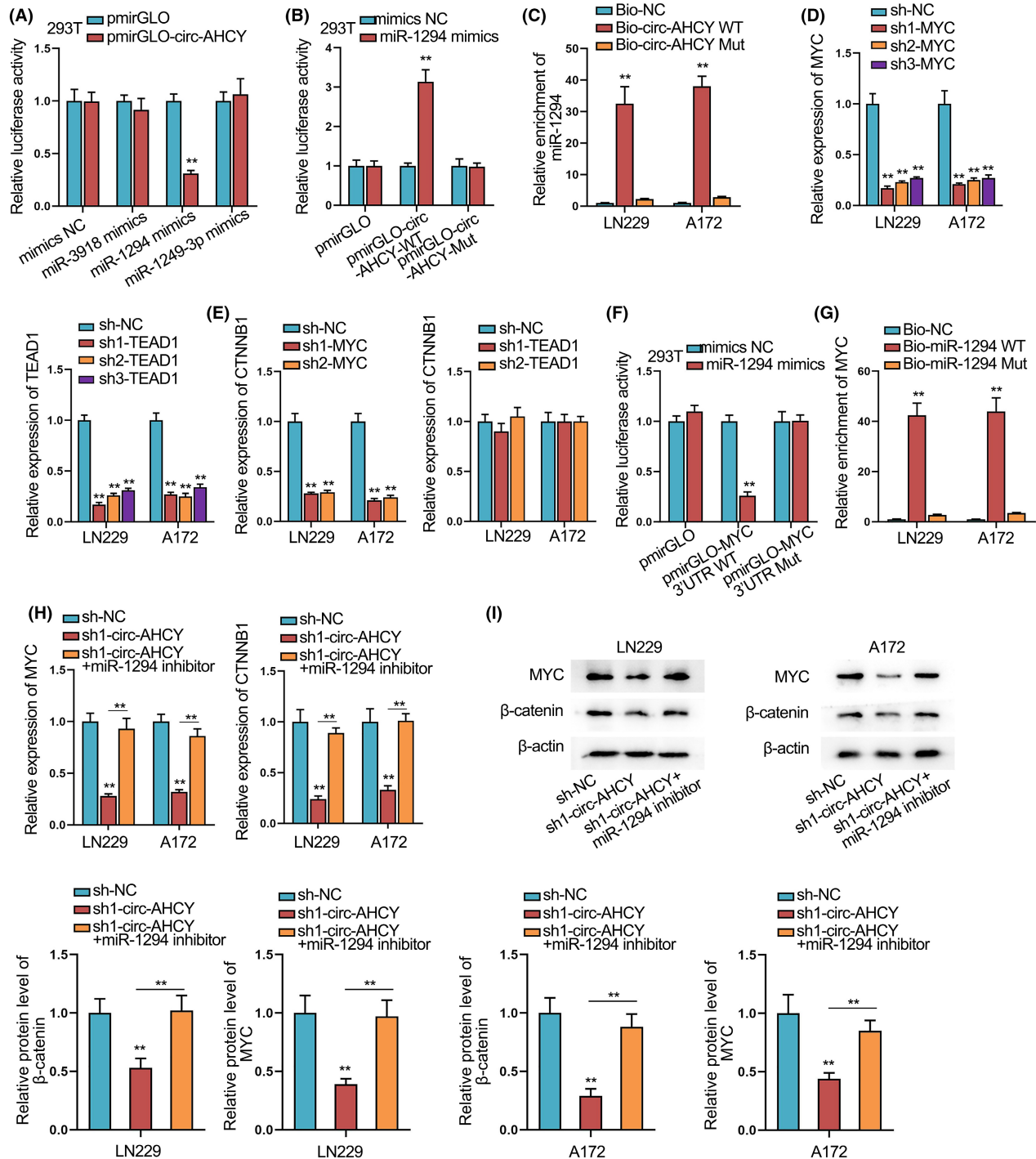


Figure 4. Circ-AHCY transcriptionally activates CTNNB1 via miR-1294/MYC axis. (A) Luciferase activity of pmirGLO-circ-AHCY in 293T cells co-transfected with overexpression plasmids of different miRNAs was analyzed. (B) Luciferase activity of pmirGLO-circ-AHCY-WT/Mut under miR-1294 mimics transfection was detected. (C) RNA pull-down assay was used to examine the interaction between miR-1294 and circ-AHCY. (D) MYC and TEAD1 was respectively knocked down in GBM cells. (E) CTNNB1 expression in response to silence of MYC or TEAD1 was detected by qRT-PCR. (F) Luciferase activity of pmirGLO-MYC 3'UTR-WT/Mut under miR-1294 mimics transfection was detected. (G) The interaction between MYC and miR-1294 was determined by RNA pull-down assay. (H) Change in MYC expression due to circ-AHCY silence or miR-1294 inhibition was detected via qRT-PCR. (I) Change in MYC and β -catenin protein levels due to circ-AHCY silence or miR-1294 inhibition was detected via west-ern blot. ** $p < 0.01$.

binding sites between miR-1294 and circ-AHCY, since the luciferase activity of circ-AHCY-Mut was hardly changed by miR-1294 up-regulation (Fig. 4B) and miR-1294 was largely enriched in Bio-circ-AHCY-WT, rather than Bio-circ-AHCY-Mut (Fig. 4C). According to starBase prediction (strict stringency ≥ 5 ; program number = 4), we also screened out potential target mRNAs binding with miR-1294. As MYC and TEAD1 have been identified to be the transcription factor,^{15,16} we chose them for the following investigation. It was indicated by qRT-PCR results that sh1/2/3-MYC and sh1/2/3-TEAD1 plasmids can effectively down-regulate the expression levels of MYC and TEAD1, respectively (Fig. 4D). Due to the higher efficiency, we used sh1/2-MYC and sh1/2-TEAD1 for the ensuing assays. With the transfection of these plasmids, we observed that only MYC knockdown led to a significant decrease of CTNNB1 (Fig. 4E), which meant that MYC might be the downstream target in circ-AHCY-centered ceRNA network and further influence CTNNB1 expression. Luciferase reporter and RNA pull-down assays revealed that miR-1294 was able to bind with MYC (Fig. 4F,G). As indicated by qRT-PCR and western blot, miR-1294 inhibition abrogated the inhibitory effect of circ-AHCY knockdown on MYC, β -catenin and CTNNB1 levels (Fig. 4H,I). Moreover, ChIP assay was performed, and we found that CTNNB1 promoter was highly enriched in Anti-MYC (Fig. S2A). Through JASPAR website (<https://jaspar.genereg.net/>), we projected the DNA binding motif of MYC and the potential binding sites of MYC on CTNNB1 promoter (Fig. S2B,C). Based on luciferase reporter assay, the luciferase activity of CTNNB1 promoter-WT was found to be significantly increased after MYC overexpression, while that of CTNNB1 promoter-Mut1+2 was hardly affected by MYC increment (Fig. S2D). These findings represented that CTNNB1 promoter was able to bind with MYC. In summary, circ-AHCY sequesters miR-1294 to up-regulate MYC, thereby further activating CTNNB1 transcription.

Circ-AHCY is transcriptionally activated by transcription factor TCF4

Through qRT-PCR, we also found that MYC depletion resulted in the down-regulation of circ-AHCY (Fig. 5A). As the binding relationship between MYC and circ-AHCY promoter was excluded (Fig. 5B), we conjectured that circ-AHCY was likely to be the downstream target of Wnt/ β -catenin signaling pathway. β -catenin has been identified to bind with TCF/LEF family of transcription factors (TCF1, TCF3, TCF4, LEF1) to form complex and to induce the expressions of downstream targets.^{17,18} According to the prediction on UCSC database (<https://genome.ucsc.edu/>), we found that TCF4 was the potential

transcription factor of circ-AHCY. Reportedly, TCF4- β -catenin transcription complex can promote tumorigenesis and tumor progression.¹⁹ The DNA motif of TCF4 and its binding sites on circ-AHCY promoter were demonstrated in Fig. 5C,D. The predicted binding sites were verified by luciferase reporter assay, as the luciferase activity of circ-AHCY promoter was elevated in response to TCF4 augment (Fig. 5E). ChIP assay re-confirmed the binding affinity between TCF4 and circ-AHCY promoter (Fig. 5F). It was illustrated by qRT-PCR data that TCF4 positively regulated circ-AHCY expression (Fig. 5G). To conclude, TCF4 mediates circ-AHCY transcription in GBM cells.

Circ-AHCY recruits EIF4A3 to up-regulate TCF4 to induce the formation of TCF4/ β -catenin complex

In this section, we firstly corroborated that TCF4 can interact with β -catenin through conducting Co-IP (Fig. 6A). As exhibited by qRT-PCR and western blot, circ-AHCY interference resulted in a decline of TCF4 mRNA and protein levels (Fig. 6B,C). RIP assay showed that circ-AHCY down-regulation made no difference to the enrichment of TCF4 in Anti-Ago2 (Fig. 6D), indicating that circ-AHCY cannot regulate TCF4 at the post-transcriptional level. CircRNAs have been uncovered to exert their functions via interaction with varied RNA binding proteins (RBPs).²⁰ After starBase prediction, we obtained a list of candidate RBPs, among which EIF4A3 has been reported to improve mRNA stability to promote malignant phenotype of cancer cells.²¹ Herein, we performed qRT-PCR and observed that EIF4A3 down-regulation contributed to a decrease of TCF4 expression (Fig. 6E). RNA pull-down and RIP assays proved the combination of EIF4A3 with circ-AHCY and TCF4 (Fig. 6F,G). Moreover, as indicated by RIP assay, the binding of EIF4A3 to TCF4 was impeded by circ-AHCY deficiency (Fig. 6H). In ActD-treated GBM cells, the degradation of TCF4 was accelerated in response to circ-AHCY or EIF4A3 depletion (Fig. 6I). To sum up, circ-AHCY decoys EIF4A3 to stabilize TCF4 to form TCF4/ β -catenin complex.

Exosomal circ-AHCY derived from GBM cells induces abnormal NHA cell growth

To explore the intercellular relationship between GBM and NHA cells, we cultured NHA cells in the culture medium (CM) of GBM cells. After cultivation, we found that NHA cell proliferation was significantly enhanced (Fig. 7A–C) and circ-AHCY expression was increased as well (Fig. 7D). Accordingly, we extracted exosomes from

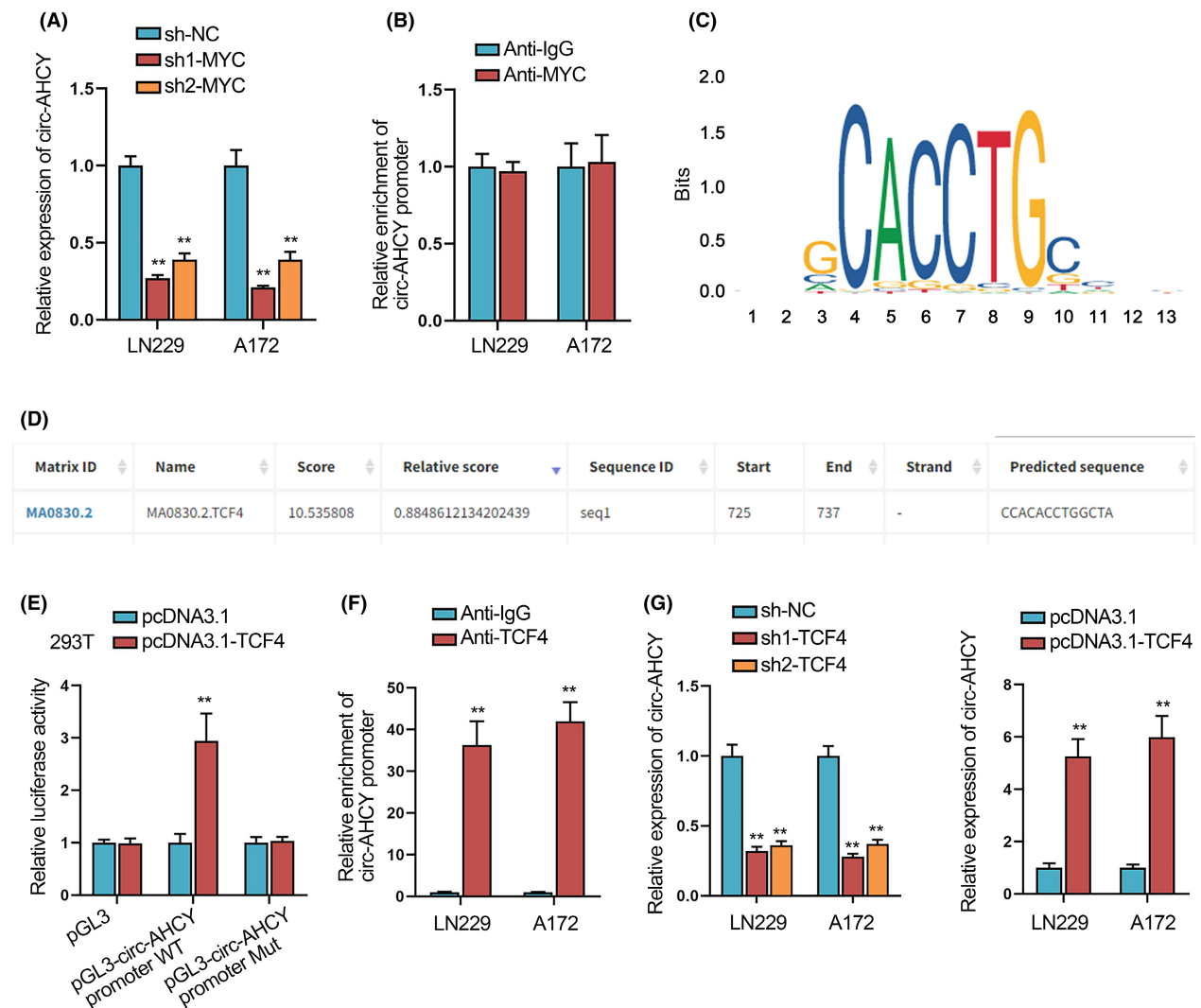


Figure 5. TCF4/β-catenin promotes the transcription of circ-AHCY. (A) Circ-AHCY expression after MYC depletion was detected via qRT-PCR. (B) Binding of circ-AHCY to MYC was analyzed by ChIP. (C and D) Binding motif of TCF4 and binding sites of TCF4 on circ-AHCY promoter was obtained from JASPAR. (E) Luciferase activity of pGL3-circ-AHCY promoter WT/Mut was detected under TCF4 augment. (F) Cohesion between circ-AHCY promoter and TCF4 was detected via ChIP. (G) Circ-AHCY expression was measured through qRT-PCR after TCF4 was silenced or over-expressed. ** $p < 0.01$.

LN229 and A172 cells and detected the levels of exosomes markers (CD63, CD81, and TSG101) using western blot (Fig. 7E). Exosomes were also labeled by PKH67 (Fig. 7F). NTA outcomes illustrated that the diameter of exosomes was 50–150 nm (Fig. 7G), which is in line with the general morphology of exosomes. As illustrated in Fig. S3A, Cy3-labeled circ-AHCY was not detected in GW4869-treated NHA cells co-cultured with LN229/Exos or A172/Exos, further proving the enrichment and secretion of circ-AHCY in LN229/Exos or A172/Exos. Moreover, we investigated the impact of GBM cell-secreted exosomal circ-AHCY on the proliferation of NHA cells. Before that, we measured the expression of circ-AHCY in

NHA cells after co-culturing with GBM cell-secreted exosomes via qRT-PCR. As qRT-PCR analysis presented, circ-AHCY expression was largely up-regulated in NHA cells co-cultured with GBM cell-secreted exosomes (Fig. 7H). The proliferation of NHA cells was facilitated after treatment of GBM cell-derived exosomes (Fig. 7I–K). All in all, exosomal circ-AHCY transmitted by GBM cells stimulates the proliferation of NHA cells.

Discussion

CircRNAs have been heatedly discussed in recent years as a regulator in the progression of diseases. CircRNA

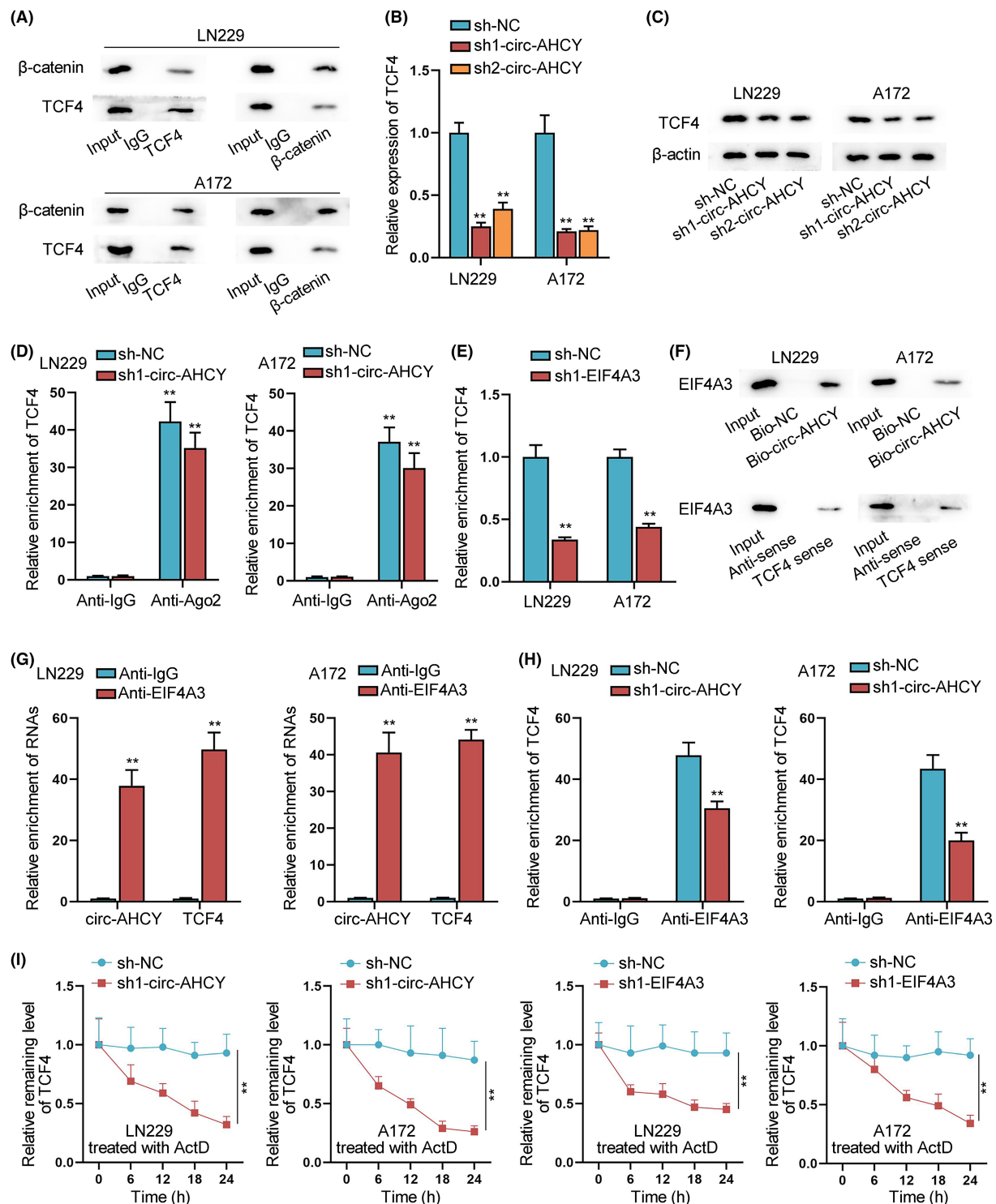


Figure 6. Circ-AHCY up-regulates TCF4 to induce the formation of TCF4/β-catenin complex. (A) Binding of TCF4 to β-catenin was analyzed via Co-IP. (B) TCF4 expression after circ-AHCY silencing was analyzed by qRT-PCR. (C) Protein level of TCF4 after circ-AHCY depletion was measured by western blot. (D) RIP assay detected TCF4 enrichment in RISC after circ-AHCY depletion. (E) TCF4 expression after EIF4A3 silencing was analyzed via qRT-PCR. (F and G) The binding of EIF4A3 with circ-AHCY and TCF4 was analyzed by RNA pull-down and RIP assays. (H) The effect of circ-AHCY knockdown on the interaction between TCF4 and EIF4A3 was analyzed by RIP assay. (I) TCF4 degradation in ActD-treated GBM cells was analyzed by qRT-PCR after circ-AHCY or EIF4A3 depletion. ** $p < 0.01$.

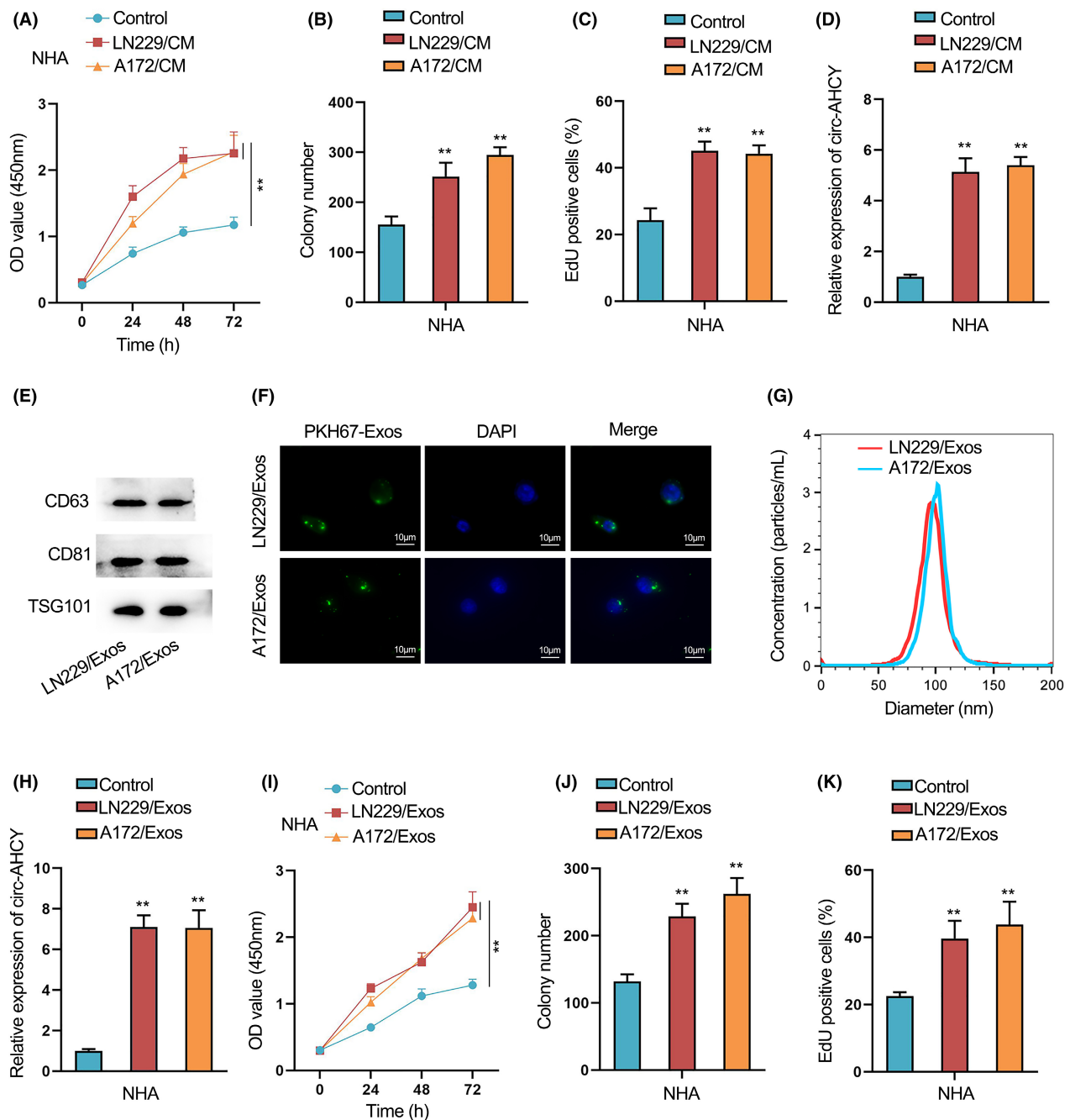


Figure 7. Exosomal circ-AHCY from GBM cells promotes malignant behaviors of NHA cells. (A–C) NHA cell proliferation was evaluated via CCK-8, colony formation and EdU assays after cultivation in CM of GBM cells. (D) Circ-AHCY expression in NHA after cultivation in CM of GBM cells was quantified via qRT-PCR. (E) Exosome markers were detected through western blot. (F) Exosomes marked by PKH67 were detected under confocal microscope. Scale bar = 10 μ m. (G) The diameter of exosomes was analyzed via NTA. (H) Circ-AHCY expression in NHA after the treatment of GBM cell-derived exosomes was quantified via qRT-PCR. (I–K) NHA cell proliferation was evaluated after the treatment of GBM cell-derived exosomes via CCK-8, colony formation and EdU assays. ** $p < 0.01$.

dysregulation has also been widely reported in GBM. Specifically, circCLSPN, circFLNA and circMELK have been identified as oncogenes in GBM.^{22–24} In this study, we uncovered a novel circRNA displaying ectopic expression

in GBM cells, namely, circ-AHCY. Both in vitro and in vivo experiments jointly revealed that circ-AHCY could induce GBM cell proliferation and exacerbate GBM tumor growth.

As to the signaling pathway through which circ-AHCY exerted influences, we found out that Wnt signaling activity was weakened in response to circ-AHCY silencing. Mediated by 19 secreted glycoproteins, Wnt signaling is a critical mediator of cell–cell communication, and the perturbations in Wnt signaling may result in the development of diseases.²⁵ Wnt signaling has been reported to be a crucial oncogenic driver in GBM.²⁶ Through experiments, it was determined that circ-AHCY could positively modulate β -catenin, the key factor of the Wnt signaling pathway, by transcriptionally activating the transcription of CTNNB1. More specifically, cytoplasmic circ-AHCY sponges miR-1294 to positively modulate MYC, the transcription factor of CTNNB1.

It is known that when Wnt signaling is activated, the accumulated β -catenin would form a complex with TCF in the nucleus, thereby inducing the transcription of target genes.²⁷ Herein, we found out that MYC depletion could also affect circ-AHCY expression. Moreover, TCF4 was predicted to be the transcription factor of circ-AHCY. Thus, we wondered whether β -catenin, which was targeted by MYC, could coordinate with TCF4 to modulate circ-AHCY transcription. Experimental results verified that TCF4 could bind with circ-AHCY promoter to activate circ-AHCY transcription.

After we confirmed the transcriptional regulation of TCF4/ β -catenin on circ-AHCY, we also noticed the regulation of circ-AHCY on TCF4. Consistently, previous study has also unveiled that circ-IQGAP1 could regulate TCF4 at post-transcriptional level by competitively binding with mi-671-5p.²⁸ However, through mechanism assays, we ruled out the possibility of ceRNA mechanism involving circ-AHCY and TCF4. Thereafter, another post-transcriptional regulatory network regarding RBP was taken into our consideration. RBPs have been repeatedly found to mediate circRNAs' maintenance of mRNA stability.^{20,29} Based on bioinformatic prediction and experiments, we confirmed that circ-AHCY could recruit EIF4A3 to maintain TCF4 mRNA stability.

In addition to the circ-AHCY regulatory axis in GBM cells, we also probed into the functional role of exosomal circ-AHCY in NHAs. Existing study has indicated that exosomes comprising various substances, including circRNAs, could be used as prognostic markers for cancer progression.³⁰ We co-cultivated NHAs with the culture medium of GBM cells so that circ-AHCY secreted by GBM cells could be transmitted by exosomes to NHAs. It was found that after co-culturing, NHA proliferation was accelerated. However, whether exosomal circ-AHCY plays its functional role in NHAs through the same regulatory axis as in GBM cells was not explicitly investigated in this study. In the future, we will further explore the mechanisms of exosomal circ-AHCY in NHAs.

In conclusion, circ-AHCY has been proved to promote GBM progression. Mechanically, circ-AHCY transcriptionally activates β -catenin through miR-1294/MYC axis to activate Wnt/ β -catenin pathway, and TCF4/ β -catenin activates circ-AHCY transcription. Meanwhile, circ-AHCY maintains TCF4 mRNA stability in an EIF4A3-dependent manner. Thus, a positive regulatory loop in GBM cells is formed.

Acknowledgments

We thank all those who participated in this study.

Author Contributions

Yuhui Li and Xuan Zheng wrote article, Jiangong Wang and Mingyang Sun designed the experiment, Dan Li and Zhuo Wang analyzed data, Jingwu Li, Yufeng Li and Yongliang Liu administrated the whole study.

Conflicts of Interest

The authors declare that they have no competing interests.

References

1. Kunadis E, Lakiotaki E, Korkolopoulou P, Piperi C. Targeting post-translational histone modifying enzymes in glioblastoma. *Pharmacol Ther.* 2021;220:107721.
2. Ou A, Yung WKA, Majd N. Molecular mechanisms of treatment resistance in glioblastoma. *Int J Mol Sci.* 2020;22(1):351.
3. Jackson CM, Choi J, Lim M. Mechanisms of immunotherapy resistance: lessons from glioblastoma. *Nat Immunol.* 2019;20(9):1100–1109.
4. Jacob F, Salinas RD, Zhang DY, et al. A patient-derived glioblastoma organoid model and biobank recapitulates inter- and intra-tumoral heterogeneity. *Cell.* 2020;180(1):188–204.e22.
5. Gao X, Xia X, Li F, et al. Circular RNA-encoded oncogenic E-cadherin variant promotes glioblastoma tumorigenicity through activation of EGFR-STAT3 signalling. *Nat Cell Biol.* 2021;23(3):278–291.
6. Chen W, Wang N, Lian M. CircRNA circPTK2 might suppress cancer cell invasion and migration of glioblastoma by inhibiting miR-23a maturation. *Neuropsychiatr Dis Treat.* 2021;17:2767–2774.
7. Yuan F, Sun Q, Xu Y, et al. Hsa_circ_0072309 inhibits proliferation and invasion of glioblastoma. *Pathol Res Pract.* 2021;222:153433.
8. Xin J, Zhang XY, Sun DK, Tian LQ, Xu P. Up-regulated circular RNA hsa_circ_0067934 contributes to glioblastoma progression through activating PI3K-AKT

- pathway. *Eur Rev Med Pharmacol Sci*. 2019;23(8):3447-3454.
9. Luo H, Yi T, Huang D, et al. circ_PTN contributes to - cisplatin resistance in glioblastoma via PI3K/AKT signaling through the miR-542-3p/PIK3R3 pathway. *Mol Ther Nucl Acids*. 2021;26:1255-1269.
 10. Qi X, Zhang DH, Wu N, Xiao JH, Wang X, Ma W. ceRNA in cancer: possible functions and clinical implications. *J Med Genet*. 2015;52(10):710-718.
 11. Du WW, Zhang C, Yang W, Yong T, Awan FM, Yang BB. Identifying and characterizing circRNA-protein interaction. *Theranostics*. 2017;7(17):4183-4191.
 12. Wang T, Mao P, Feng Y, et al. Blocking hsa_circ_0006168 suppresses cell proliferation and motility of human glioblastoma cells by regulating hsa_circ_0006168/miR-628-5p/IGF1R ceRNA axis. *Cell Cycle (Georgetown, Tex)*. 2021;20(12):1181-1194.
 13. Li W, Wang S, Shan B, et al. CircHECTD1 regulates cell proliferation and migration by the miR-320-5p/SLC2A1 Axis in glioblastoma multiform. *Front Oncol*. 2021;11:666391.
 14. Koritzinsky EH, Street JM, Star RA, Yuen PS. Quantification of exosomes. *J Cell Physiol*. 2017;232(7):1587-1590.
 15. Luo Z, Liu X, Xie H, Wang Y, Lin C. ZFP281 recruits MYC to active promoters in regulating transcriptional initiation and elongation. *Mol Cell Biol*. 2019;39(24):e00329-19.
 16. Wen T, Liu J, He X, et al. Transcription factor TEAD1 is essential for vascular development by promoting vascular smooth muscle differentiation. *Cell Death Differ*. 2019;26(12):2790-2806.
 17. Du L, Lee JH, Jiang H, et al. β -Catenin induces transcriptional expression of PD-L1 to promote glioblastoma immune evasion. *J Exp Med*. 2020;217(11):e20191115.
 18. Robinson KF, Narasipura SD, Wallace J, Ritz EM, Al-Harthi L. β -Catenin and TCFs/LEF signaling discordantly regulate IL-6 expression in astrocytes. *Cell Commun Signal*. 2020;18(1):93.
 19. Han P, Li JW, Zhang BM, et al. The lncRNA CRNDE promotes colorectal cancer cell proliferation and chemoresistance via miR-181a-5p-mediated regulation of Wnt/ β -catenin signaling. *Mol Cancer*. 2017;16(1):9.
 20. Chen J, Wu Y, Luo X, et al. Circular RNA circRHOTB3 represses metastasis by regulating the HuR-mediated mRNA stability of PTBP1 in colorectal cancer. *Theranostics*. 2021;11(15):7507-7526.
 21. Lu C, Rong D, Hui B, et al. CircETFA upregulates CCL5 by sponging miR-612 and recruiting EIF4A3 to promote hepatocellular carcinoma. *Cell Death Discov*. 2021;7(1):321.
 22. Hu T, Lei D, Zhou J, Zhang BO. circRNA derived from CLSPN (circCLSPN) is an oncogene in human glioblastoma multiforme by regulating cell growth, migration and invasion via ceRNA pathway. *J Biosci*. 2021;46:66.
 23. Sun Y, Ma G, Xiang H, et al. circFLNA promotes glioblastoma proliferation and invasion by negatively regulating miR-199-3p expression. *Mol Med Rep*. 2021;24(5):786.
 24. Zhou F, Wang B, Wang H, et al. circMELK promotes glioblastoma multiforme cell tumorigenesis through the miR-593/EphB2 axis. *Mol Ther Nucl Acids*. 2021;25:25-36.
 25. Guan R, Zhang X, Guo M. Glioblastoma stem cells and Wnt signaling pathway: molecular mechanisms and therapeutic targets. *Chin Neurosurg J*. 2020;6:25.
 26. Shahcheraghi SH, Tchokonte-Nana V, Lotfi M, Lotfi M, Ghorbani A, Sadeghnia HR. Wnt/ β -catenin and PI3K/Akt/mTOR signaling pathways in glioblastoma: two Main targets for drug design: a review. *Curr Pharm des*. 2020;26(15):1729-1741.
 27. Cho GW, Kim MH, Kim SH, et al. TCF/ β -catenin plays an important role in HCCR-1 oncogene expression. *BMC Mol Biol*. 2009;10:42.
 28. Xi P, Zhang CL, Wu SY, Liu L, Li WJ, Li YM. CircRNA circ-IQGAP1 knockdown alleviates interleukin-1 β -induced osteoarthritis progression via targeting miR-671-5p/TCF4. *Orthop Surg*. 2021;13(3):1036-1046.
 29. Chen RX, Chen X, Xia LP, et al. N(6)-methyladenosine modification of circNSUN2 facilitates cytoplasmic export and stabilizes HMGA2 to promote colorectal liver metastasis. *Nat Commun*. 2019;10(1):4695.
 30. Dai J, Su Y, Zhong S, et al. Exosomes: key players in cancer and potential therapeutic strategy. *Signal Transduct Target Ther*. 2020;5(1):145.

Supporting Information

Additional supporting information may be found online in the Supporting Information section at the end of the article.

Figure S1.

Figure S2.

Figure S3.